Materials Science and Engineering C 58 (2016) 1138–1149

Contents lists available at ScienceDirect

Materials Science and Engineering C

journal homepage: www.elsevier.com/locate/msec

Modified silk fibroin scaffolds with collagen/decellularized pulp for bone tissue engineering in cleft palate: Morphological structures and biofunctionalities

Supaporn Sangkert [a], Jirut Meesane [a,*], Suttatip Kamonmattayakul [b], Wen Lin Chai [c]

[a] Biological Materials for Medicine Research Unit, Faculty of Medicine, Institute of Biomedical Engineering, Prince of Songkla University, Hat Yai, Songkhla90110, Thailand
[b] Faculty of Dentistry, Department of Preventive Dentistry, Prince of Songkla University, Hat Yai, Songkhla90110, Thailand
[c] Faculty of Dentistry, Department of General Dental Practice and Oral and Maxillofacial Imaging, University of Malaya, Kuala Lumpur, Malaysia

ARTICLE INFO

Article history:
Received 14 April 2015
Received in revised form 16 July 2015
Accepted 7 September 2015
Available online 12 September 2015

Keywords:
Silk fibroin
Tissue engineering
Collagen
Decellularized pulp
Osteoblast

ABSTRACT

Cleft palate is a congenital malformation that generates a maxillofacial bone defect around the mouth area. The creation of performance scaffolds for bone tissue engineering in cleft palate is an issue that was proposed in this research. Because of its good biocompatibility, high stability, and non-toxicity, silk fibroin was selected as the scaffold of choice in this research. Silk fibroin scaffolds were prepared by freeze-drying before immerging in a solution of collagen, decellularized pulp, and collagen/decellularized pulp. Then, the immersed scaffolds were freeze-dried. Structural organization in solution was observed by Atomic Force Microscope (AFM). The molecular organization of the solutions and crystal structure of the scaffolds were characterized by Fourier transform infrared (FT-IR) and X-ray diffraction (XRD), respectively. The weight increase of the modified scaffolds and the pore size were determined. The morphology was observed by a scanning electron microscope (SEM). Mechanical properties were tested. Biofunctionalities were considered by seeding osteoblasts in silk fibroin scaffolds before analysis of the cell proliferation, viability, total protein assay, and histological analysis. The results demonstrated that dendrite structure of the fibrils occurred in those solutions. Molecular organization of the components in solution arranged themselves into an irregular structure. The fibrils were deposited in the pores of the modified silk fibroin scaffolds. The modified scaffolds showed a beta-sheet structure. The morphological structure affected the mechanical properties of the silk fibroin scaffolds with and without modification. Following assessment of the biofunctionalities, the modified silk fibroin scaffolds could induce cell proliferation, viability, and total protein particularly in modified silk fibroin with collagen/decellularized pulp. Furthermore, the histological analysis indicated that the cells could adhere in modified silk fibroin scaffolds. Finally, it can be deduced that modified silk fibroin scaffolds with collagen/decellularized pulp had the performance for bone tissue engineering and a promise for cleft palate treatment.

1. Introduction

Cleft palate is a congenital malformation that develops from a defect in facial development. This defect includes bone loss around the mouth. Cleft palate causes dysfunction of the mouth, for instance, problematic verbal and speech development, and abnormal suction during breast sucking (1). To treat cleft palate, patients need to have an operation. However, incomplete bone tissue regeneration often occurs post-operatively. Therefore, creating a potential approach to complete the bone regeneration is a challenge for cleft palate.

Bone tissue engineering is the process of regeneration of functional tissue. Bone tissue engineering can treat bone tissue defects from disease (2). Principally, tissue engineering is an interdisciplinary field that includes three disciplines: material engineering, cell technology, and biomaterials (3). Biomaterials for tissue engineering scaffolds are especially important to induce bone tissue regeneration (4).

Silk fibroin (SF) is a protein that is produced by the *Bombyx mori* silkworm. The main proteins of silk fibroin include the amino acids glycine (43%), alanine (30%), and serine (12%) (5). Importantly, silk fibroin can arrange into three forms: (1) random coil, (2) alpha helix, and (3) crystalline β-sheet. The properties of silk fibroin are slow degradation, biocompatibility, low immunogenicity and toxicity, and good mechanical properties. Silk-based biomaterials were used as tissue engineering scaffolds in skeletal tissue like bone, cartilage, connective skin, and ligament tissue (6). Particularly in bone tissue engineering, the silk fibroin scaffold is a suitable choice because it has stability during bone tissue regeneration (7).

Collagen is a natural protein that is the main component in the extracellular matrix (ECM) in tissue. Especially in bone tissue, collagen acts as

* Corresponding author.
E-mail address: jirutmeesane999@yahoo.co.uk (J. Meesane).

http://dx.doi.org/10.1016/j.msec.2015.09.031
0928-4931/

Table 1
Groups of silk scaffolds coated with the coating solutions.

Group	Detail
A	Silk scaffold
B	Silk-coated decellularized pulp
C	Silk-coated collagen
D	Silk-coated collagen and decellularized pulp

the template for calcium phosphate deposition. More specifically, collagen can enhance the stability and strength of the bone (8). Collagen is a popular material for tissue regeneration because collagen has biofunctionalities that cells can recognize. Such functionalities can enhance cell adhesion that leads to inducing tissue regeneration (9).

Pulp is the tissue located in teeth that has an ECM in its texture (10). Generally, this ECM plays a significant role as a native scaffold for bone tissue regeneration (11). Some reports demonstrated the performance of ECM from different sources for bone tissue regeneration (12). Normally, isolating ECM is an important step before it is used for tissue regeneration. Therefore, decellularized tissue is an attractive approach which has been used to isolate ECM. However, the use of decellularized pulp in bone tissue engineering has been rarely reported. Hence, the use of decellularized pulp is the proposed novel choice for bone tissue engineering in this research.

Due to the attractiveness of collagen and decellularized pulp, we developed a high performance silk fibroin scaffold by modification with collagen/decellularized pulp for application in cleft palate. The hybridization of collagen with decellularized pulp was considered and prepared in a solution. Silk fibroin scaffolds were coated with that solution. The characterization of the morphological structure and biofunctionalities were considered in this research. The eventual aim of this research was to enhance the biofunctionalities of a porous silk scaffold with collagen/decellularized pulp for bone tissue engineering in cleft palate.

2. Materials and methods

2.1. Preparation of silk fibroin scaffolds

Silk fibrin scaffolds were prepared by boiling the cocoons for 30 min in 0.02 M Na_2CO_3 and then rinsed with distilled water to extract the sericin. The silk was dried in a hot air oven at 60 °C for 24 h. The silk was dissolved in a 9.3 M LiBr solution at 70 °C for 3 h and then a silk solution was prepared yielding a 3% (w/v) solution (13). After dissolving the silk fibroin, it was centrifuged for 20 min at 9000 RPM at 4 °C (14). The silk solution was purified by dialyzing against distilled water for 3 days (15). The silk fibroin solution was stored at 4 °C until further use. Preparation of the 3D silk scaffold for experiment followed five steps. First, the silk fibroin solution was poured in 48-well plates. Second, the silk fibroin solution was freeze-dried to generate the porosity. Third, the porous silk scaffolds were treated by immersion in 70% (v/v) methanol for 30 min. Fourth, porous silk scaffolds were freeze-dried again. Finally, all scaffolds were cut into a diameter of 10 mm and 2 mm in thickness.

2.2. Preparation of type I collagen

Type I collagen was extracted from the skin of brown banded bamboo shark (*Chiloscyllium punctatum*). The preparation of type I collagen followed the report of P. Kittiphattanabawon et al. 2010 (16). Briefly, shark skin (1.0×10 cm^2) was mixed with 0.1 M NaOH. Next, the deproteinized skin was soaked in 0.5 M acetic acid for 48 h. After filtering the mixture to get the collagen solution, NaCl was added to a final concentration of 2.6 M and 0.05 M Tris (hydroxymethyl) aminomethane at pH 7.5. The pellet was dissolved in a minimum volume of 0.5 M acetic acid and the collagen pellet was collected following refrigerated centrifugation. For a more purified collagen solution, dialysis was performed with 0.1 M acetic acid for 12 h and 48 h with distilled water. The freeze-dried method was used to remove the water and it was kept at −20 °C for later use.

2.3. Preparation of decellularized pulp

We collected teeth pulp from children who were 6 to 10 years old and segmented the teeth in half to harvest the pulp tissue. Collagenase and dispase were used to digest the pulp into solution for 1 h. The solution was separated from the debris pellet by using a centrifuge at 37 °C. Then, the solution was washed with PBS (phosphate-buffered saline) 2 times. Finally, the solution was filtered to get the decellularized pulp and used the freeze-drying machine for water sublimation (17).

2.4. Modification of silk fibroin scaffolds

For modification of silk fibroin scaffolds, we designed the silk fibroin scaffolds into 4 groups that were modified with different coating solutions (Table 1). For coated silk scaffolds in the decellularized pulp group, the decellularized pulp powder was dissolved in 0.1% sodium hypochlorite to a concentration of 0.1 mg/ml. In the case of coated silk scaffolds with collagen, the collagen powder was dissolved in 0.1 M acetic acid to a concentration of 0.1 mg/ml (18). For coated silk scaffolds with collagen/decellularized pulp, the previous collagen and decellularized pulp were mixed together to obtain a 50:50 ratio. The collagen, decellularized pulp, and collagen/decellularized pulp were used as the coating solutions to modify the scaffolds. To modify the scaffolds, the silk fibroin scaffolds were immersed into the coating solutions for 240 min. Then, the immersed scaffolds were soaked in 1× PBS for 30 min before they were freeze-dried (19).

2.5. Pore size measurement

The ImageJ software (1.48v) was used to measure the pore size in each group. The pore distribution of the scaffolds was analyzed from

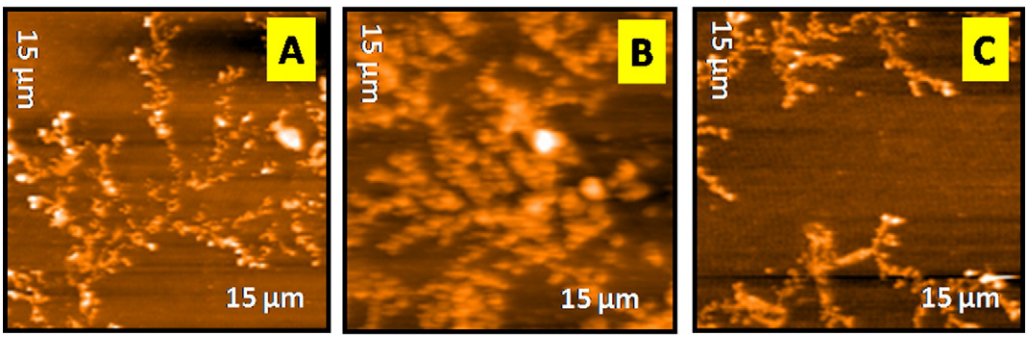

Fig. 1. AFM images of structure formation of coating solution: (A) decellularized pulp, (B) collagen, and (C) collagen/decellularized pulp.

SEM images. The pore size of the scaffolds in each group was a randomized area ($n = 25$) to calculate the average pore size (20).

2.6. Weight increase of the modified scaffolds

The weight increase of the modified scaffolds was measured by the percentage deposition of components in the coating solution on the scaffolds. All groups of silk scaffold were weighed before and after coating ($n = 5$). The difference in the weights showed the increased percentages of the components from the coating solutions that attached onto the silk scaffolds (21). The calculation for the percentage deposition of components in the coating solution onto the scaffold (w/w, %) was $(W_t - W_p) / W_t \times 100\%$, where W_t = weight of the coated scaffold and W_p = weight of scaffold.

2.7. Swelling testing

The silk scaffolds in all groups were soaked in PBS at 37° C for 24 h. After removal of excess PBS by contact with a plastic surface, the swollen samples were weighed immediately. The swelling ratios were calculated using the equation $(W_s - W_d)/W_d$, where W_s and W_d are the weights of the swollen scaffold and the dry scaffold, respectively (22).

2.8. Mechanical properties testing

The mechanical properties of the scaffolds in the wet phase were investigated using the Universal Testing Machine (Lloyd model LRX-Plus, Lloyd Instrument Ltd., London, UK). In this study, all groups of scaffolds were cut into a diameter of 10 mm and a thickness of 5 mm. The testing machine used a static load cell of 10 N at a rate of 2 mm/min and stopped at a strain of 40%.

2.9. Fourier transform infrared (FT-IR) characterization

The molecular organization of the silk fibroin scaffolds and the silk fibroin scaffolds coated with decellularized pulp, collagen, and collagen/decellularized pulp were analyzed by FT-IR. The samples were analyzed as a KBr pellet in an FT-IR spectrophotometer using the EQUINOX 55 (Bruker Optics, Germany) in the range of 4000–400 cm^{-1}.

2.10. X-ray diffraction (XRD) characterization

The crystal structure of the silk fibroin scaffolds and silk fibroin scaffolds coated with decellularized pulp, collagen, and collagen/decellularized pulp were analyzed by XRD (X'Pert MPD (PHILIPS, Netherlands). Samples were put in the XRD instrument and the diffraction patterns were measured over a 2 θ range of 5–90 θ with a step size of 0.05 θ and time per step of 1 s.

2.11. Scanning electron microscopy (SEM) observations

A scanning electron microscope (Quanta400, FEI, Czech Republic) was used to observe the morphology and characterization of the SF scaffold that was coated with a special solution. The samples were precoated with gold using a gold sputter coater machine (SPI Supplies, Division of STRUCTURE PROBE Inc., Westchester, PA USA).

3. Atomic force microscopy observations

The coating solution for each group was dropped into a glass slide, smeared, and soaked in PBS for 30 min. When the slides were dried, the morphology and structure were observed by using atomic force microscopy (Nanosurf easyScan 2 AFM, Switzerland).

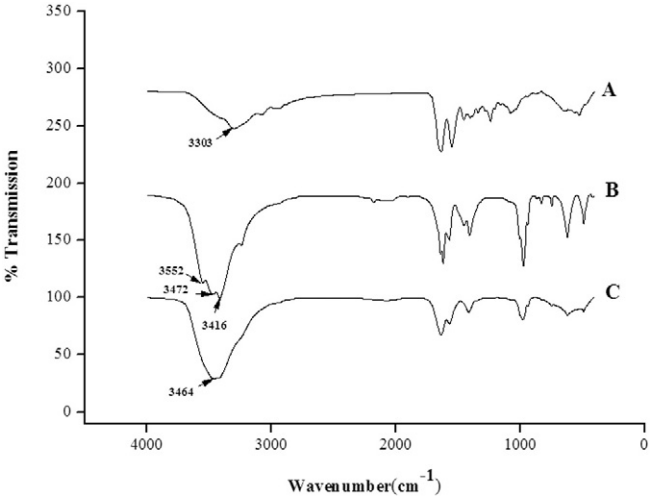

Fig. 2. FT-IR spectra: (A) collagen, (B) decellularized pulp, and (C) collagen/decellularized pulp.

3.1. Cell culture experiments

The MG-63 cell line was cultured in alpha-MEM medium (α-MEM, Gibco™, Invitrogen, Carlsbad, CA) with the addition of 1% penicillin/streptomycin, 0.1% fungizone, and 10% fetal bovine serum (FBS) at 37 °C in a humidified CO_2 (5%) and air (95%) incubator. The MG-63 was seeded with a 5×10^5/silk scaffold and the medium was changed every 3–4 days (23). The osteogenic medium (10 mM b-glycerophosphate, 50 mg = mL ascorbic acid, and 100 nM dexamethasone; Sigma-Aldrich) was used for osteoblast differentiation of MG-63 (24).

3.2. Cell proliferation assay (PrestoBlue: Day 1, 3, 5, and 7)

To observe the cell proliferation, PrestoBlue assay was used based on resazurin reagent. When the live cells go through the reducing process in the cytoplasm they will react with the resazurin to form resorufin to produce a purple or red color. The measurement of cell proliferation was performed according to the manufacturer's instructions (PrestoBlue® Cell Viability Reagent, Invitrogen, USA) and measured at 1, 3, 5, and 7 days (25). Silk fibroin scaffolds from each group were

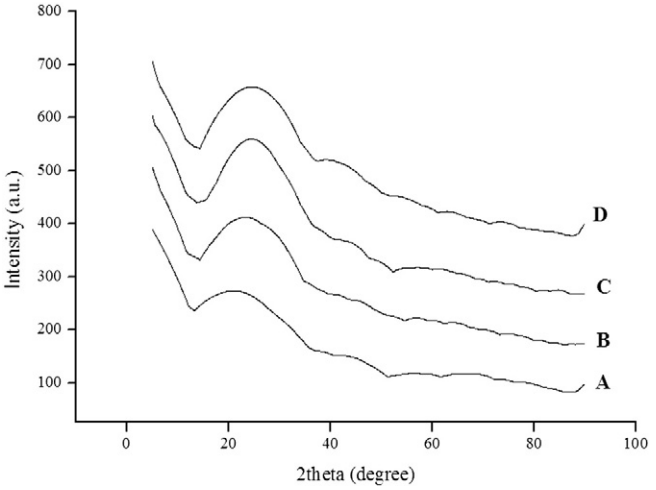

Fig. 3. XRD spectra: (A) silk fibroin scaffold, (B) silk fibroin scaffold coated with decellularized pulp, (C) silk fibroin scaffold coated with collagen, and (D) silk fibroin scaffold coated with collagen/decellularized pulp.

washed twice with 1× PBS and then 1/10th volume of PrestoBlue reagent was added directly into the complete media and incubated for 1 h at 37 °C and the proliferation rate of the cells was measured by monitoring the wavelength absorbance at 600 nm emission. The untreated cell group was used for the negative control.

3.3. Cell viability (fluorescence microscope on day 3)

Cell viability on silk fibroin scaffold in each group was evaluated by fluorescence microscope. The live cells on the SF scaffold were stained by fluorescein diacetate (FDA). The application of the FDA was to attach to the cells and embed them into the ECM and cellular clusters. FDA was dissolved in acetone at 5 mg/ml. Next the media was removed by replacement of fresh 1 ml medium and then 5 μl of the FDA was added to each well and kept in the dark at 37 °C for 5 min. The silk fibroin scaffold was washed twice with 1× PBS and transferred to a glass slide and the cell morphology was observed by the fluorescence microscope (26).

3.4. Total protein assay

The cellular protein in the cell lysis solution was discharged according to the manufacturer's instructions (Pierce BCA Protein Assay Kit, Thermo Scientific, USA). In order to extract cellular protein by using the lysis cell method, 800 μl of the cell lysis solution (1% Triton X in PBS) was added in each well and the silk fibroin scaffolds were frozen at −70 °C for 1 h and then thawed at room temperature for 1 h. This was repeated in 3 cycles. Following that, the solution was transferred to an Eppendorf tube and centrifuged at 12000 RPM for 10 min to remove the supernatant from the pellet. The measurement of the total protein synthesized by the cells in the silk fibroin scaffold was performed with absorbance at 562 nm at 7, 14, and 21 days. Bovine serum albumin was used for the standard curve in this experiment (27).

3.5. Histology analysis

The silk fibroin scaffolds with cell cultures on day 5 were fixed with 4% formaldehyde at 4 °C for 24 h. The silk fibroin scaffolds in each group were immersed in paraffin. The paraffin sections were cut at 5 μ and placed on a glass slide and deparaffinized and hydrated in distilled water. The sample slides were stained with 2 types of stain. At first, hematoxylin and eosin stain was used to observe cell migration, adhesion, and the ECM synthesized from the cells around the silk fibroin scaffold (28).

3.6. Statistical analysis

All data were shown as mean ± standard deviation. The samples were measured and statistically compared by one-way ANOVA and Tukey's HSD test (SPSS 16.0 software package). $P < 0.05$ was accepted as statistically significant.

4. Results and discussion

4.1. Structural formation of mimicked extracellular matrix

In this research, a coating solution of collagen/decellularized pulp was prepared according to the above protocol before observation of its organization by AFM. The characterization of the structure of the collagen/decellularized pulp was the preliminary demonstration before coating onto the silk fibroin scaffolds. Furthermore, this demonstration could relate to the arrangement of the collagen/decellularized pulp on the silk fibroin scaffolds. The structure of collagen/decellularized pulp showed dendrite formation of fibrils (Fig. 1). Collagen without decellularized pulp organized predominantly into a dense branch structure. As reported previously, collagen molecules formed themselves into a fibril structure (29). Notably, collagen formed dendrite formation of fibrils when it was observed by AFM. This result can be explained by the disturbance of the collagen molecules by the sodium hypochlorite in

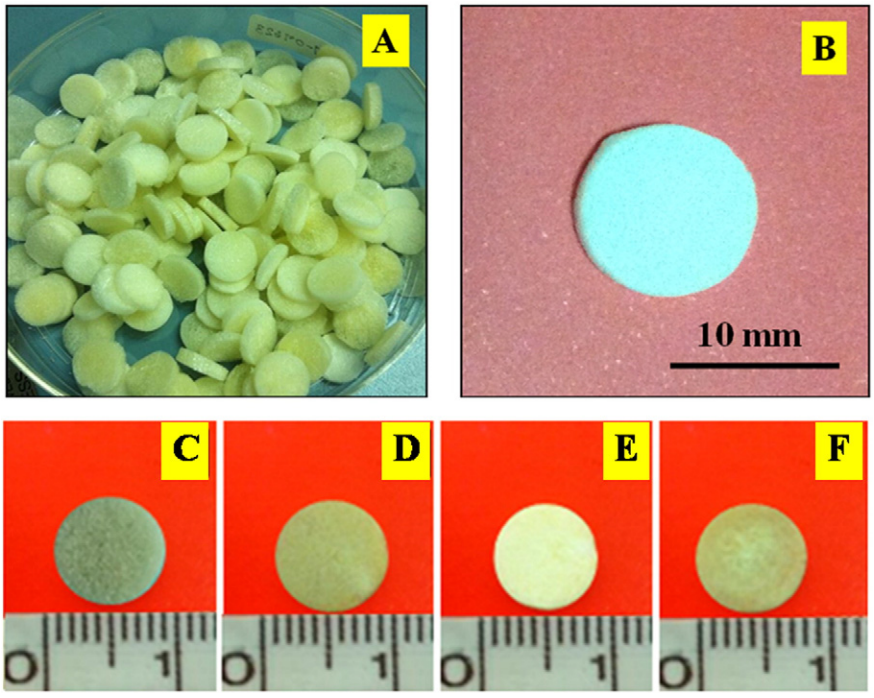

Fig. 4. Images of silk fibroin scaffolds: (A, C) before immersion (10 mm diameter × 2 mm thickness), (D) silk fibroin scaffold coated with decellularized pulp, (E) silk fibroin scaffold coated with collagen, and (B, F) silk fibroin scaffold coated with collagen/decellularized pulp.

the solution. Generally, sodium hypochlorite is a chemical reagent used for dental treatment. Sodium hypochlorite maintains fibroblast viability and promotes healing of chronic wounds (30). Some reports demonstrated that sodium hypochlorite can change hydroxyproline into pyrrole-2-carboxylic acid (31). Such forms of collagen might influence the organization into dendrite formation of fibrils.

4.2. Molecular organization analysis of modified silk fibroin scaffolds

FT-IR was used to analyze the molecular organization of the coating solutions for characterization in this research. The results of the molecular organization showed different wave numbers of the samples (Fig. 2). As previously mentioned for the collagen, the FT-IR spectrum showed the important peak of –OH groups at 3500 cm^{-1} (32,33). In this research, the –OH groups of collagen appeared at a wave number of 3303 cm^{-1} that shifted to a lower wave number. This indicated that the –OH groups interacted with the other groups. This interaction came from the self-assembly of the collagen molecules, which showed that they could organize themselves into a higher order structure. The wave number of the –OH groups in the coated silk fibroin scaffolds shifted to a higher wave number. This result indicated that the –OH groups could vibrate freely in the decellularized pulp and collagen/decellularized pulp that came from an irregular organization of the components. The decellularized pulp showed three peaks at 3416, 3472, and 3552 cm^{-1}, which represented the combination of –OH groups in each component of the decellularized pulp. The collagen/

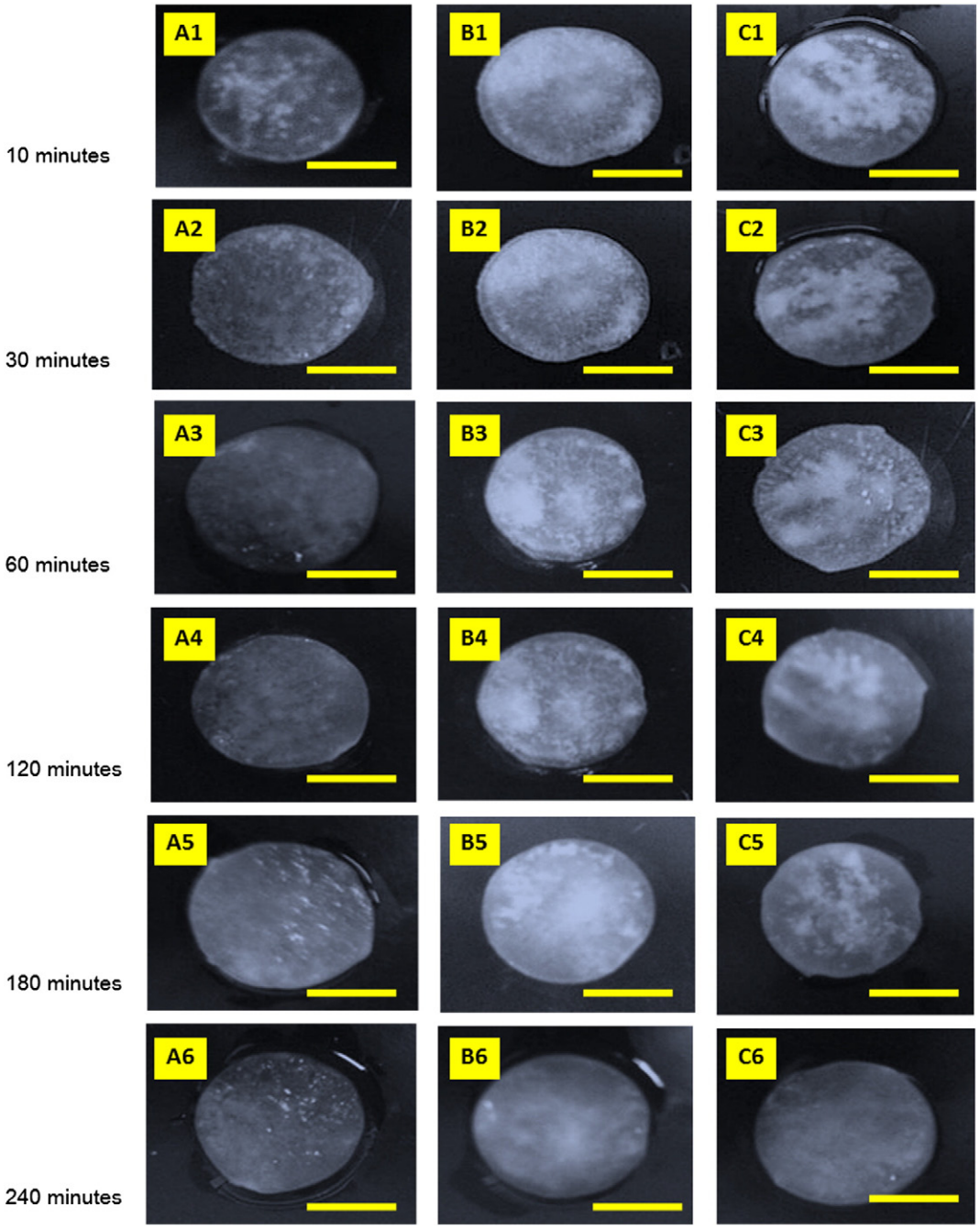

Fig. 5. Images of silk scaffolds after immersion in a coating solution at each time point of 10, 30, 60, 120, 180, and 240 min of decellularized, collagen, and collagen/decellularized solutions: (A1–A6) silk scaffold immersed with decellularized pulp solution, (B1–B6) silk scaffold immersed with collagen solution, and (C1–C6) silk scaffold immersed with collagen/decellularized pulp solution. Scale bar: 5 mm.

decellularized pulp showed –OH groups at 3464 cm^{-1} that possibly was the merged peak of collagen and decellularized pulp. Furthermore, it demonstrated that the –OH groups in the collagen/decellularized pulp could vibrate freely.

4.3. Crystal structure analysis of modified silk fibroin scaffolds

For an analysis of the crystal structure of silk fibroin scaffolds, the peak of NaCl deposited during coating was subtracted. The results showed different peaks in the crystal structures of the silk fibroin scaffolds (Fig. 3). Interestingly, the peaks that showed at around 20 degrees represented the beta-sheet conformation of silk fibroin as reported in previous literature (34). As a result, the peaks of the silk fibroin scaffold and the coated silk fibroin scaffolds appeared at around 20 degrees. This indicated that the silk fibroin scaffold and the coated silk fibroin scaffolds could organize into a beta-sheet structure.

4.4. Morphological analysis of modified silk fibroin scaffolds

In this research, silk fibroin scaffolds were modified by these coating solutions: collagen, decellularized pulp, and collagen/decellularized pulp. To start the modification, silk fibroin scaffolds were prepared by the freeze-dried technique before immersion into one of the coating solutions. Then, the immersed scaffolds were soaked in a buffer solution and then freeze-dried. The samples are shown in Fig. 4.

Observations of the uptake of the coating solutions inside the silk fibroin scaffolds during immersing are shown in Fig. 5. Silk fibroin scaffolds with decellularized pulp, collagen, and collagen/decellularized pulp showed turbid and transparent parts distributed throughout the texture of the scaffold during the early period of the immersion. The turbid and transparent parts appeared to be merged into a homogenous texture. Obviously, the apparent homogenous texture in the scaffold showed the uptake of the solution inside the scaffold. At 60 min, the decellularized pulp solution had diffused into the whole texture of the silk fibroin scaffold (Fig 5A3). For the silk fibroin scaffolds with collagen and collagen/decellularized pulp, the apparent homogenous texture appeared throughout the inside of the silk fibroin scaffold at 240 min. It could be explained that collagen and collagen/decellularized pulp had higher viscosities when compared to decellularized pulp. This result demonstrated that the solution had the potential to modify silk fibroin scaffolds by the coating technique. After immersion of the silk fibroin scaffolds in the coating solution, they were soaked in PBS before freeze-drying. Then, the morphologies of the freeze-dried modified silk fibroin scaffolds were observed by SEM (Figs. 6 and 7).

The surface morphology of silk fibroin scaffolds with and without modification showed porous structures (Fig. 6). The silk fibroin scaffold without modification showed a smooth surface of the porous walls, which had an interconnective porous structure. This interconnective porous structure is suitable to support cell adhesion and migration (35). Interestingly, cells could connect with each other in the pores. Furthermore, the pores are suitable for media flow in and out of the silk fibroin scaffold. A porous silk fibroin scaffold can easily remove waste (35). Notably, the morphologies of modified silk fibroin scaffolds with collagen (Fig. 6C) and collagen/decellularized pulp (Fig. 6D) solutions, showed the fibril structure deposited at the inner pores of the silk fibroin scaffolds. This fibril structure might be formed according to the results from AFM observation. Notably, there were no deposited fibril structures in the decellularized pulp solution. This result indicates that the decellularized pulp possibly detached from the surface of silk fibroin scaffolds while soaking in the buffer solution.

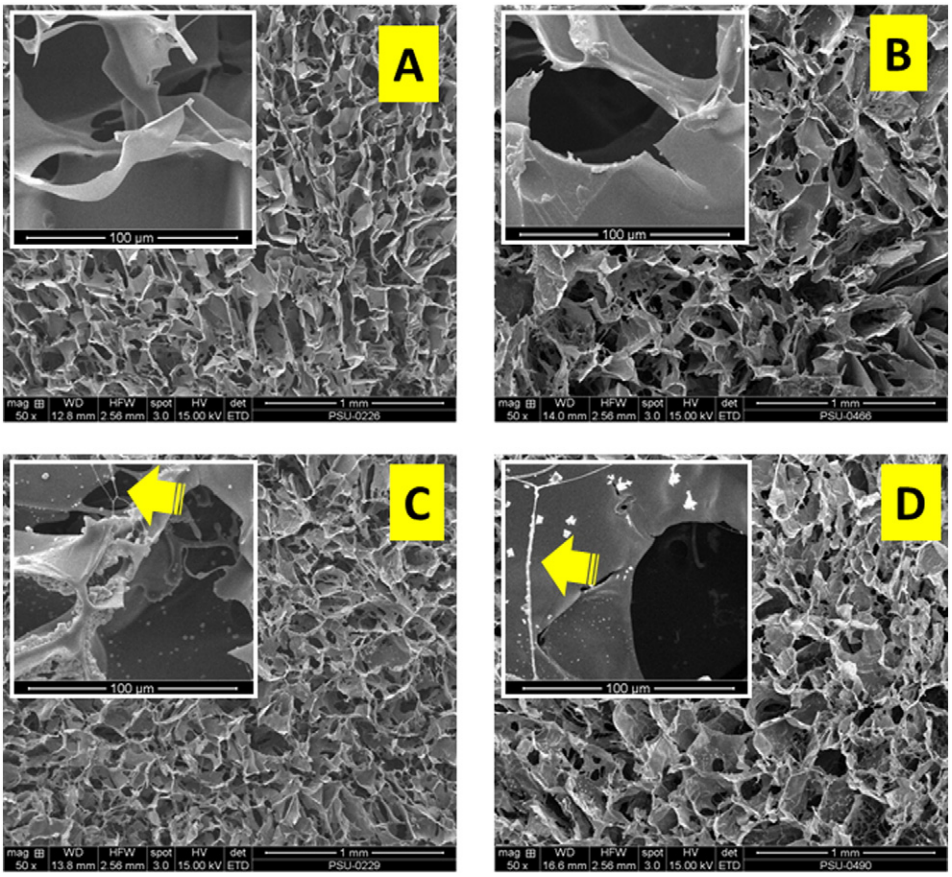

Fig. 6. Surface morphology of the scaffolds observed by scanning electron microscope (SEM) with different magnification. The wall surface is shown at 500× and connective pore size is shown at 50×. (A) surface morphology of silk scaffold without coating, (B) surface morphology of silk scaffold coated with decellularized pulp, (C) surface morphology of silk scaffold coated with collagen, and (D) surface morphology of silk scaffold coated with collagen/decellularized pulp. Scale bars are shown in the micrographs. Yellow arrows show fibril structure.

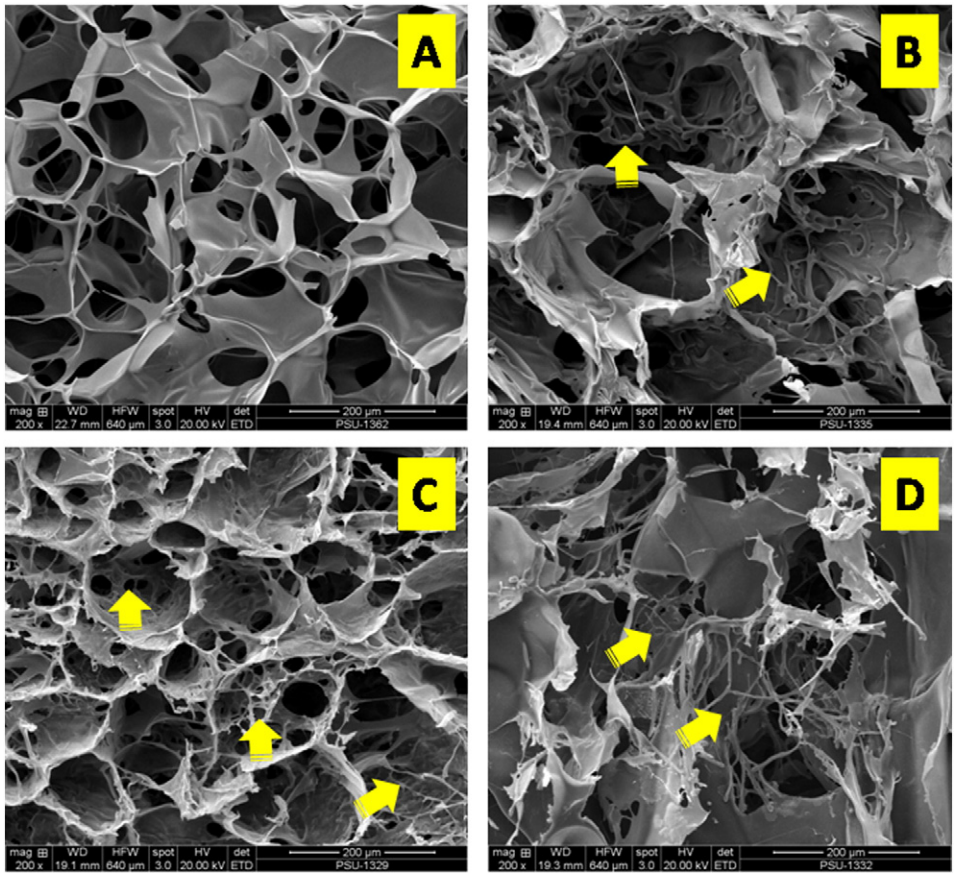

Fig. 7. Cross-sectional morphology of scaffolds observed by scanning electron microscope (SEM): (A) silk scaffold without coating, (B) silk scaffold coated with decellularized pulp, (C) silk scaffold coated with collagen, and (D) silk scaffold coated with collagen/decellularized pulp. Scale bars are shown in the micrographs. Yellow arrows show fibril structure.

Cross sections of the silk fibroin scaffolds were observed by SEM to confirm the deposition of decellularized pulp and collagen/decellularized pulp solutions inside the porous scaffolds (Fig. 7). Unlike the surface morphology of modified silk fibroin scaffold, the cross-sectional morphology showed a deposited fibril structure inside the pores of the silk fibroin scaffolds for all coating solutions. The fibrils organized themselves into a network structure that was deposited on the pore walls of the silk fibroin scaffold. It demonstrated that decellularized, collagen, and collagen/decellularized solution have the potential for use as a coating solution for modification of the silk fibroin scaffolds. These results indicate that solutions of collagen, decellularized pulp, and collagen/decellularized pulp had the ability to mimic a network structure as in an ECM.

4.5. Pore size measurement

In this research, the ImageJ software (1.48v) was used to measure the pore size in each group. The pore distribution of the scaffolds was analyzed from the SEM images. The pore size of the scaffolds in every group was a randomized area. The average pore sizes of the silk scaffolds in all groups are shown in Table 2. The mean pore size of the silk scaffolds was 132.06 ± 3.74 μm, which was the biggest pore size of all the groups but not significantly different. A minimum pore size of 100 μm with interconnective pores is normally required for a cell culture system that can support the cell size and migration (35).

Table 2
Average pore size of silk scaffold in each group. ImageJ software measured the silk scaffolds. Values are average ± standard derivation ($n = 25$).

Groups	Pore size
A: Silk scaffold	132.06 ± 3.74 μm
B: Silk scaffold coating with decellularized pulp	126.85 ± 2.72 μm
C: Silk scaffold coating with collagen	127.94 ± 1.98 μm
D: Silk scaffold coating with collagen and decellularized pulp	125.83 ± 1.98 μm

4.6. Weight increase of the modified scaffolds

To confirm the existence of collagen and collagen/decellularized pulp on silk fibroin scaffold, the percentage of weight increase was analyzed. The results showed that the modified silk fibroin scaffolds had a significantly increased weight than the silk fibroin scaffold without modification (Fig. 8). It demonstrated that decellularized pulp, collagen, and collagen/decellularized pulp could deposit and exist in the silk fibroin scaffolds. The modified silk fibroin scaffolds with collagen showed a significantly increased weight compared to either silk scaffold modified decellularized pulp and collagen/decellularized pulp. The results indicate that the solutions of decellularized pulp, collagen, and collagen/decellularized pulp can adhere onto the silk fibroin scaffolds. These results support the previous results by SEM.

4.7. Swelling ratio analysis

The scaffolds in all groups were swollen in different percentages. The uncoated scaffold showed a higher water binding capacity. This property plays an important role in tissue regeneration. (36). The silk scaffold revealed the highest water binding capacity and was significantly different than both the silk scaffold coated with decellularized pulp and the silk scaffold coated with collagen/decellularized pulp (Fig. 9). The collagen coating and the collagen/decellularized pulp on the silk scaffold surfaces seemed to decrease in the swelling ratio. The morphological structures of the silk fibroin scaffolds coated with collagen and the

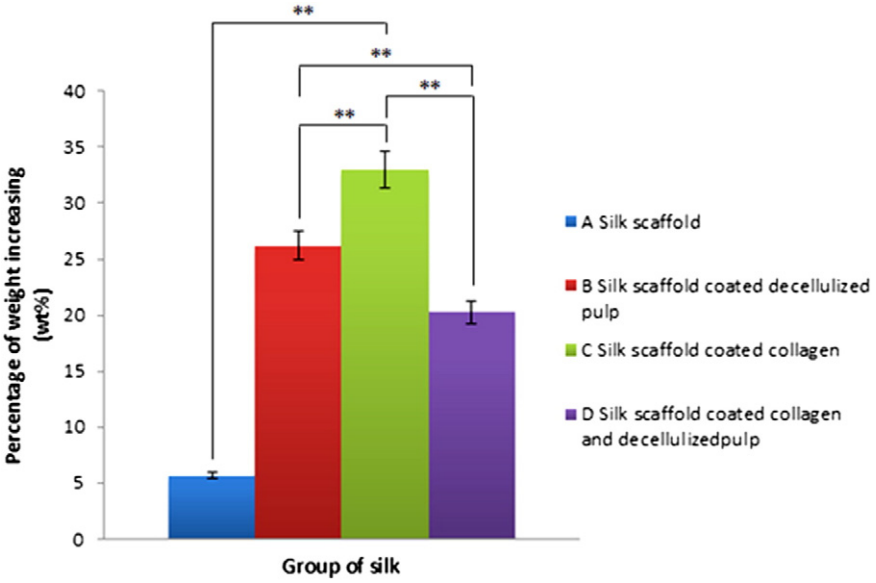

Fig. 8. Weight increase in percentage of deposition of decellularized pulp, collagen, and combination of collagen with decellularized pulp (**$P < 0.01$).

scaffolds coated with collagen/decellularized pulp had fibril network structures in the pores. These fibril networks decreased the swelling ratios. The results were similar to a previous study that reported the swelling property of the sponge-like matrices was dependent on the network porous structure and microstructure of the scaffold (37).

4.8. Mechanical testing analysis

The results in mechanical testing showed that the silk fibroin scaffold and silk fibroin coated with decellularized pulp had higher stress values at the maximum load and higher Young's moduli than the silk fibroin scaffolds coated with collagen and collagen/decellularized pulp (Fig. 10). The results indicated that coating solutions affected the mechanical properties of the silk fibroin scaffolds. The coated samples showed smaller pore sizes than the samples without a coating. The small pore sizes retained smaller amounts of water than the large pore sizes according to the results in the pore measurement and swelling ratio analyses. The water in the porous scaffolds could resist the compressive force while testing in the wet state. Therefore, the scaffolds that could hold a higher amount of water in the porous structure showed higher stress values and Young's moduli. Notably, the silk fibroin scaffold coated with decellularized pulp showed the highest stress value and Young's moduli. The morphological structure of the decellularized pulp possibly reinforced the silk fibroin scaffold.

4.9. Cell proliferation

PrestoBlue™ was used to evaluate cell proliferation on days 1, 3, 5, and 7. The proliferation of osteoblast cells continuously increased from day 1 to day 5 and became lower on culture day 7 among all groups. On day 1, the silk scaffold modified by decellularized pulp was significantly higher in cell numbers than the silk scaffold without modification (Fig. 11). On day 3, all groups showed a similar behavior of cell proliferation, except the silk scaffold modified with collagen/decellularized pulp, which was significantly higher than the other groups. On day 5, all groups became low, but the silk scaffold modified with decellularized pulp was significantly different than the other groups. On day 7, all groups had higher cell proliferation than the silk scaffold without modification.

Significantly, the results of cell proliferation indicated that decellularized pulp induced cell proliferation because the decellularized pulp had components of ECM. Importantly, the ECM could enhance cell proliferation (38). Modified silk fibroin scaffold with collagen/decellularized pulp showed the potential to enhance cell proliferation.

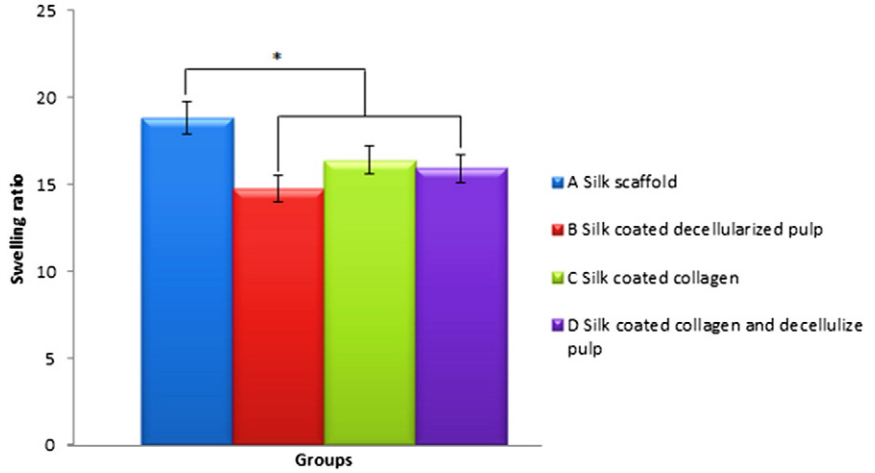

Fig. 9. Scaffold swelling ratios in each group.

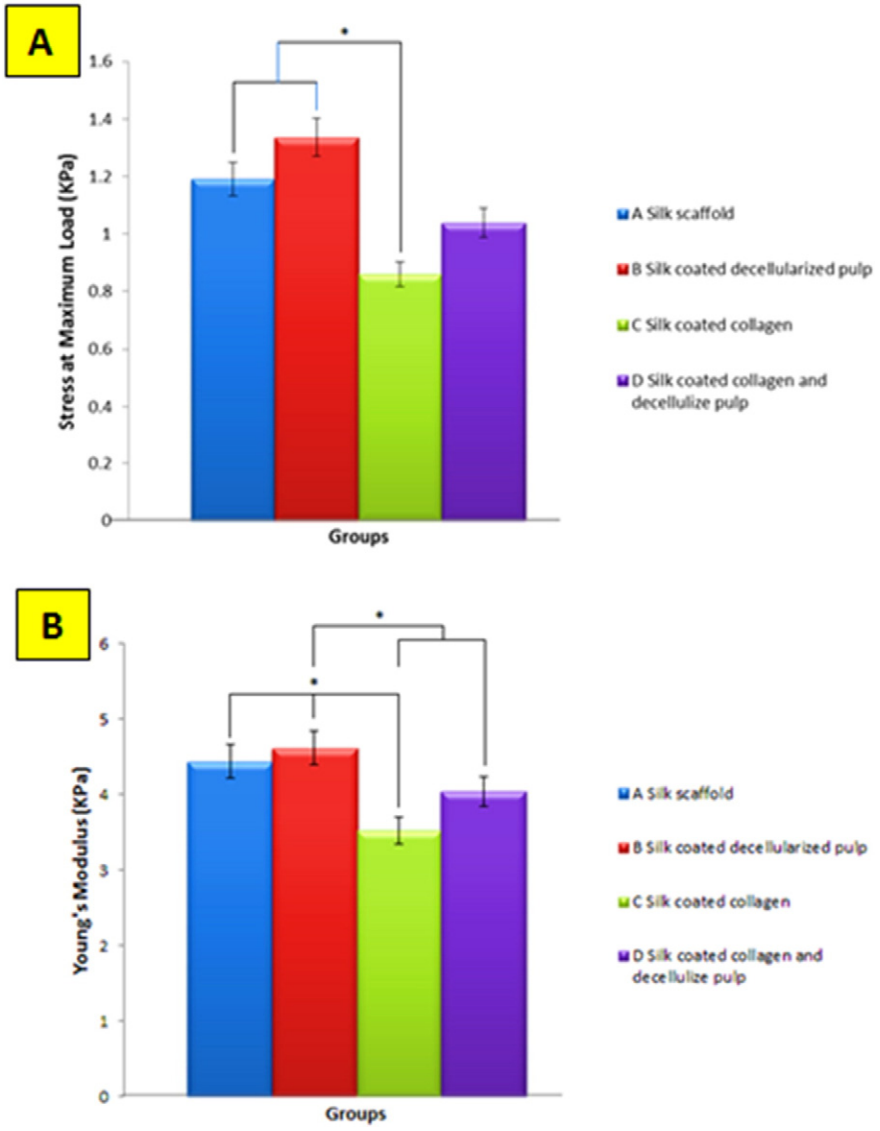

Fig. 10. Mechanical properties of the scaffolds in each group. (A) stress at maximum load of scaffold and (B) Young's modulus (KPa).

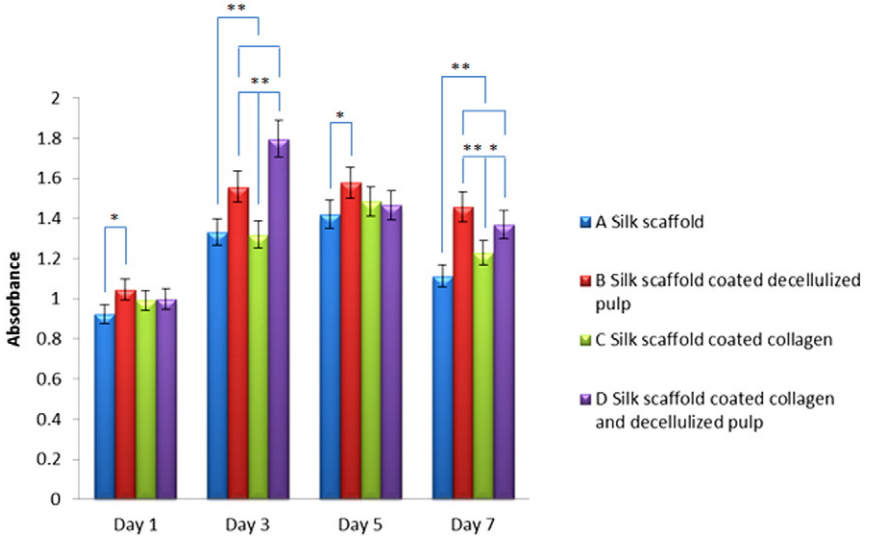

Fig. 11. Cell proliferation on different silk fibroin scaffolds. Cell proliferation was evaluated based on the associative number of metabolically active osteoblast cells in each scaffold group identified by the PrestoBlue™ assay. Significant changes in resazurin activity of osteoblasts: $^{*}P < 0.05$, $^{**}P < 0.01$.

A previous report demonstrated that collagen acted as an ECM to induce cell attachment (39). Therefore, to combine collagen with decellularized pulp can synergize cell adhesion and proliferation. From these results, collagen/decellularized pulp might be formed as reconstructed ECM that has the biofunctionalities of native ECM. Hence, such reconstructed ECM has the effect of a high cell proliferation rate.

4.10. Fluorescein diacetate (FDA)

To observe the cell morphology in scaffolds, osteoblasts were stained by FDA. Afterward, all samples were observed by a fluorescence microscope. The green luminance showed the nucleus of the osteoblasts. The osteoblasts were able to attach to the surface of silk scaffolds (Fig. 12). The cells in the modified silk scaffold with collagen/decellularized pulp arranged themselves into a dense aggregation. This result indicated that collagen/decellularized pulp can promote cell adhesion. Cell adhesion might have come from the reconstructed ECM of collagen/decellularized pulp as previously explained.

4.11. Bicinchoninic acid (BCA) analysis

Analysis of the total protein content during cell culturing was determined by BCA analysis on days 7, 14, and 21 (Fig. 13). For days 7 and 14, the modified silk scaffold with collagen had the highest protein content than the other groups. As previously reported, this demonstrated that the osteoblasts start synthesizing protein on day 7 (40). Therefore, at days 7 and 14 the modified silk scaffold with collagen showed higher protein content than the other samples. These results indicate that the protein content at days 7 and 14 came from two main parts: (1) coated collagen on the scaffold and (2) secreted collagen from the osteoblasts. This confirmed the previous results that the protein content in the modified scaffold with collagen is higher than the other samples. The protein content at day 21 of the modified silk fibroin scaffold with collagen/decellularized pulp was predominantly higher than the other samples. On day 21, the silk fibroin scaffold coated with collagen/decellularized pulp and the silk fibroin scaffold coated with decellularized pulp continuously showed higher synthesizing of protein. On the other hand, protein synthesizing in the silk fibroin scaffold and silk scaffold coated with collagen became low at day 21. These results demonstrated that the coated components on modified silk fibroin scaffolds with collagen/decellularized pulp had a unique role in promoting the synthesizing of protein. It indicated that the biofunctionalities of collagen and decellularized pulp could synergize protein.

4.12. Histological analysis

Osteoblast cells showed a good distribution throughout the silk scaffold in all groups. In Fig. 14, the red arrows point at the silk scaffold

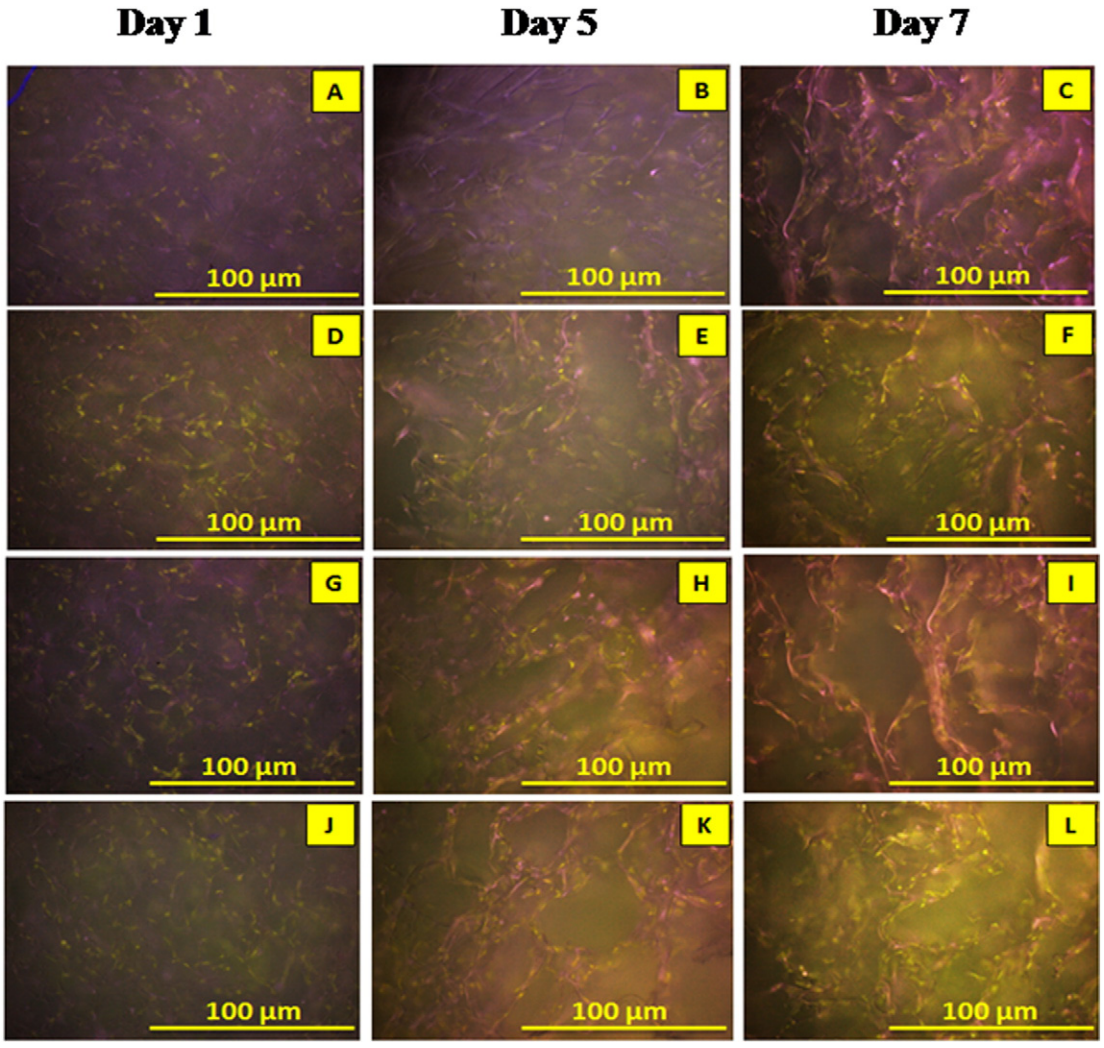

Fig. 12. Fluorescence images of the obvious cells and interconnections of the osteoblast cells on the silk scaffolds (FDA label, green brightness). (A–C) silk scaffold, (D–F) silk scaffold coated with decellularized pulp, (G–I) silk scaffold coated with collagen, (J–L) silk scaffold coated with collagen/decellularized pulp.

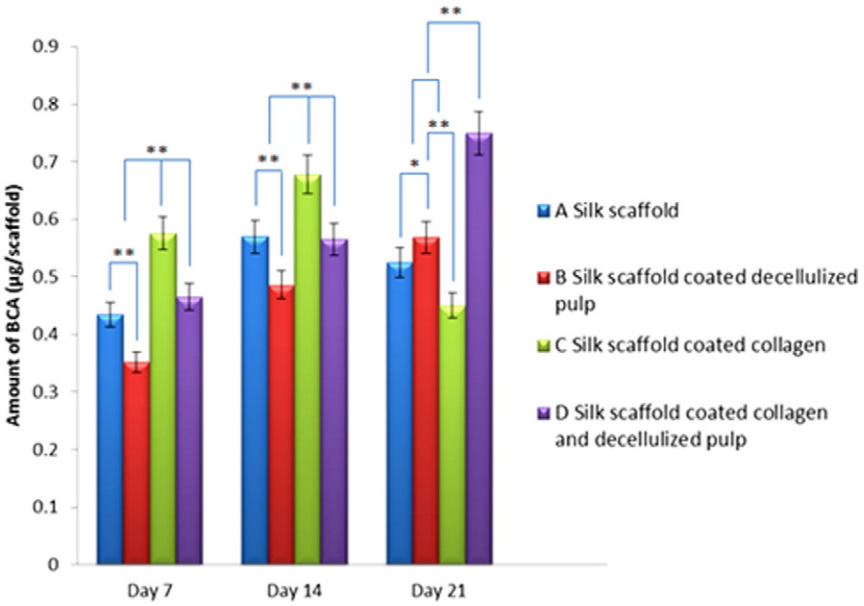

Fig. 13. Total protein content of osteoblast cells (MG63) on silk scaffold. Protein synthesis was evaluated by using the Pierce BCA protein assay. Significant changes in protein activity of osteoblasts: $^{*}P < 0.05$, $^{**}P < 0.01$.

and the yellow arrows point at the osteoblast cells attached to the silk scaffold. The silk-coated scaffolds with decellularized pulp (Fig. 14B), collagen (Fig. 14C), and collagen/decellularized pulp (Fig. 14D) showed more osteoblast cells attached to the surface of the silk scaffold and the cells filled the pores of the scaffolds. The shape of the osteoblast cells was flat on the silk scaffold surface and the blue color indicates the nucleus that is located at the center of the cytoplasm. These results indicated that modified silk fibroin scaffold could induce cell adhesion.

5. Conclusion

This research demonstrated that the use of collagen, decellularized pulp, and collagen/decellularized pulp solutions for scaffold modification is attractive and is a potential approach to enhance the biofunctionalities of silk fibroin scaffolds. The solutions could organize themselves into fibrils that deposited in the pores of the silk fibroin scaffolds. More importantly, the results indicated that the fibrils in modified

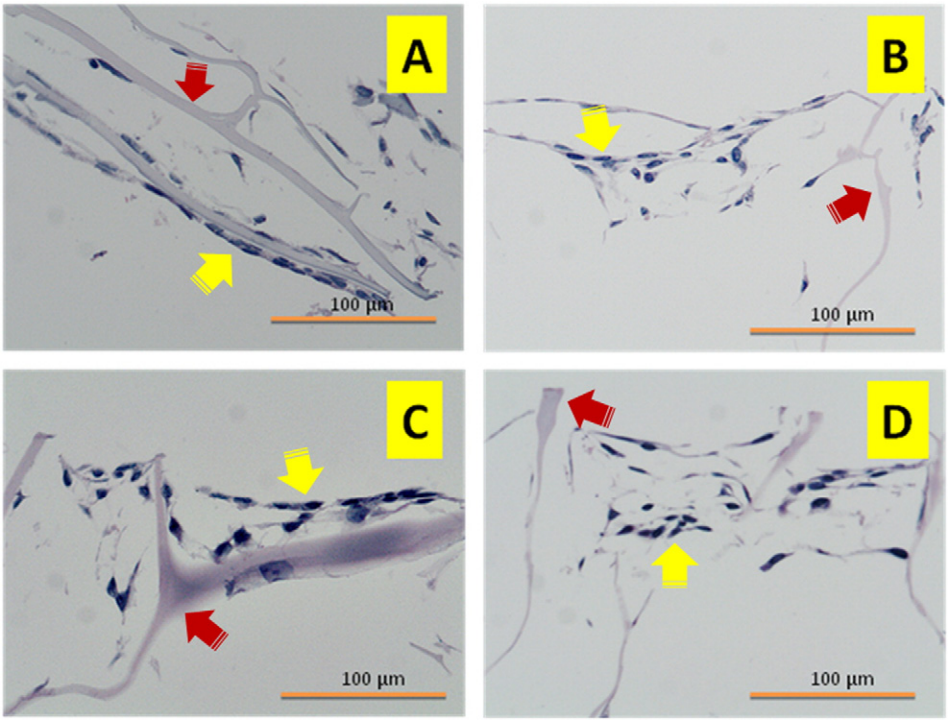

Fig. 14. Hematoxylin and eosin staining of cross sections on day 5 (A, B, C, D); the red arrows show the silk scaffold in each group, the yellow arrows show the osteoblast cells attached to the silk scaffold in all groups: (A) silk scaffold, (B) silk scaffold coated with decellularized pulp, (C) silk fibroin coated with collagen, and (D) silk fibroin coated with collagen/decellularized pulp. Scale bar: 100 µm.

silk fibroin scaffolds can induce biofunctionalities including cell proliferation, cell viability, and protein synthesis. Furthermore, the histological analysis demonstrated that cells could adhere well to the modified silk fibroin scaffolds. Interestingly, it indicated that the modified silk fibroin scaffolds coated with collagen/decellularized pulp had a unique structure and demonstrated biofunctionalities. The structure and biofunctionalities could enhance the performance of modified silk fibroin scaffold. Eventually, it can be deduced from these results that modified silk fibroin scaffolds coated with collagen/decellularized pulp has promise for use in bone tissue engineering particularly in cleft palate.

Acknowledgment

This work was financially supported by grant no. EC 50-042-25-2-3 from the Faculty of Medicine, Prince of Songkla University. Many thanks to the Biological Materials for Medicine (BMM) Research Unit and Queen Sirikit Sericulture Centre, Narathiwat, for silk supporting.

References

[1] P.A. Zuk, Tissue engineering craniofacial defects with adult stem cells? Are We Ready Yet. Pediatric Research. 63 (2008) 478–486.
[2] G.M. de Peppoa, I. Marcos-Campos, D. John Kahler, D. Alsalman, L. Shang, G. Vunjak-Novakovic, D. Marolt, Engineering bone tissue substitutes from human induced pluripotent stem cells, PNAS. 110 (2013) 8680–8685.
[3] R. Langer, J.P. Vacanti, Tissue Engineering, Science. 260 (1993) 920–926.
[4] F.J. O'Brien, J.P. Vacanti, Biomaterials & scaffolds for tissue engineering, 14 (2011) 88–95.
[5] Z. Zhao, Y. Li, M.B. Xie, Silk fibroin-based nanoparticles for drug delivery, Int J Mol Sci. 16 (2015) 4880–4903.
[6] Y. Wang, D.J. Blasioli, H.J. Kim, H.S. Kim, D.L. Kaplan, Cartilage tissue engineering with silk scaffolds and human articular chondrocytes, Biomaterials. 27 (2006) 4434–4442.
[7] B. Kundu, R. Rajkhowa, S.C. Kundu, X. Wang, Silk fibroin biomaterials for tissue regenerations, Advanced Drug Delivery Reviews. 65 (2013) 457–470.
[8] T. Matsuura, K. Tokutomi, M. Sasaki, M. Katafuchi, E. Mizumachi, H. Sato, Distinct characteristics of mandibular bone collagen relative to long bone collagen: relevance to clinical dentistry, BioMed Research International. 2014 (2014) 1–9.
[9] G.E. Davis, Affinity of integrins for damaged extracellular matrix: αvβ3 binds to denatured collagen type I through RGD sites, Biochemical and Biophysical Research Communications 182 (1992) 1025–1031.
[10] M. Goldberg, J. Smith, Cells and extracellular matrices of dentin and pulp: a biological basis for repair and tissue engineering, Crit Rev Oral Biol Med. 15 (2004) 13–27.
[11] L. Cen, W. Liu, L. Cui, W. Zhang, Y. Cao, Collagen tissue engineering: development of novel biomaterials and applications, Pediatric Research. 63 (2008) 492–496.
[12] S. Yamada, K. Yamamoto, T. Ikeda, K. Yanagiguchi, Y. Hayashi, Potency of fish collagen as a scaffold for regenerative medicine, BioMed Research International. 2014 (2014) 1–8.
[13] G. Chang, H.-J. Kim, D.L. Kaplan, G. Vunjak-Novakovic, R.A. Kandel, Porous silk scaffolds can be used for tissue engineering annulus fibrosus, Eur Spine J. 16 (2007) 1848–1857.
[14] L.P. Yan, J. Silva-Correia, C. Correia, S.G. Caridade, E.M. Fernandes, R.A. Sousa, J.F. Mano, J.M. Oliveira, A.L. Oliveira, R.L. Reis, Bioactive macro/micro porous silk fibroin/nano-sized calcium phosphate scaffolds with potential for bone-tissue-engineering applications, Nanomedicine. 8 (2013) 359–378.
[15] Y. Zhao, R.Z. Legeros, J. Chen, Initial study on 3D porous silk fibroin scaffold: preparation and morphology, Bioceramics Development and Applications. 1 (2011) 1–3.
[16] P. Kittiphattanabawon, S. Benjakul, W. Visessanguan, H. Kishimura, F. Shahidi, Isolation and characterisation of collagen from the skin of brownbanded bamboo shark (*Chiloscyllium punctatum*), Food Chemistry. 119 (2010) 1519–1526.
[17] S.B. Traphagen, N. Fourligas, J. Xylas, S. Sengupta, D. Kaplan, I. Georgakoudi, P.C. Yelick, Characterization of natural, Decellularized and Reseeded Porcine Tooth Bud Matrices. Biomaterials. 33 (2012) 5287–5296.
[18] A. Gigante, S. Manzotti, C. Bevilacqua, M. Orciani, R. Di Primio, M. Mattioli-Belmonte, Adult mesenchymal stem cells for bone and cartilage engineering: effect of scaffold materials, European Journal of Histochemistry. 52 (2008) 169–174.
[19] K. Chen, S. Sahoo, P. He, K.S. Ng, S.L. Toh, J.L. Goh, A hybrid Silk/RADA-based fibrous scaffold with triple hierarchy for ligament regeneration, Tissue Eng: Part A. 18 (2012) 1399–1409.
[20] N. Kasoju, D. Kubies, M.M. Kumorek, J. Krız, E. Fabryova, L. Machova, J. Kovarova, F. Rypacek, Dip TIPS as a facile and versatile method for fabrication of polymer foams with controlled shape size and pore architecture for bioengineering applications, PLoS ONE. 9 (2014) 1–16.
[21] P. He, S. Sahoo, K.S. Ng, K. Chen, S.L. Toh, J.C.H. Goh, Enhanced osteoinductivity and osteoconductivity throughhydroxyapatite coating of silk-based tissue-engineeredligament scaffold, Biomedical Materials Research Part A. 101A (2013) 555–566.
[22] N. Guziewicza, A. Besta, B. Perez-Ramireza, D.L. Kaplanb, Lyophilized silk fibroin hydrogels for the sustained local delivery of therapeutic monoclonal antibodies, Biomaterials. 32 (2011) 2642–2650.
[23] X. Liu, M. Zhao, J. Lu, J. Ma, J. Wei, S. Wei, Cell responses to two kinds of nanohydroxyapatite with different sizes and crystallinities, International Journal of Nanomedicine. 7 (2012) 1239–1250.
[24] B.S. Kim, H.J. Kang, J. Lee, Improvement of the compressive strength of a cuttlefish bone-derived porous hydroxyapatite scaffold via polycaprolactone coating, Journal of Biomedical Materials Research Part B: Applied Biomaterials. 101 (2013) 1302–1309.
[25] H. Liu, L. Xia, Y. Dai, M. Zhao, Z. Zhou, H. Liu, Fabrication and characterization of novel hydroxyapatite/porous carbon composite scaffolds, Materials Letters. 66 (2011) 36–38.
[26] T.T. Li, K. Ebert, J. Vogel, T. Groth, Comparative studies on osteogenic potential of micro- and nanofibre scaffolds prepared by electrospinning of poly(ε-caprolactone), Progress in Biomaterials. 2 (2013) 1–13.
[27] F. Pati, H. Kalita, B. Adhikari, S. Dhara, Comparative studies on osteogenic potential of micro- and nanofibre scaffolds prepared by electrospinning of poly(ε-caprolactone), Progress in Biomaterials. 2 (2013) 1–13.
[28] M.B. Keogh, F.J. O' Brien, J.S. Daly, A novel collagen scaffold supports human osteogenesis applications for bone tissue engineering, Cell and Tissue Research 340 (2010) 169–177.
[29] D.E. Birk, E.I. Zycband, D.A. Winkelmann, R.L. Trelstad, Collagen fibrillogenesis in situ: fibril segments are intermediates in matrix assembly, Proc. Nati. Acad. Sci. USA 86 (1989) 4549–4553.
[30] Century Pharmaceuticals, Inc., Diluted Dakin's Solution Support for Antisepsis of Chronic Wounds.
[31] J.A. Beeley, H.K. Yip, A.G. Stevenson, Conservative dentistry: chemochemical caries removal: a review of the techniques and latest developments, British Dental Journal. 188 (2000) 427–430.
[32] A. John, L. Hong, Y. Ikada, Y. Tabata, A trial to prepare biodegradable collagen-hydroxyapatite composites for bone repair, J Biomater Sci Polym Ed. 12 (2001) 689–705.
[33] O.S. Rabotyagova, P. Cebe, D.L. Kaplan, Collagen structural hierarchy and susceptibility to degradation by ultraviolet radiation, Mater Sci Eng C Mater Biol Appl. 28 (2008) 1420–1429.
[34] M. Farokhi, F. Mottaghitalab, J. Hadjati, R. Omidvar, M. Majidi, A. Amanzadeh, M. Azami, S.M. Tavangar, M.A. Shokrgozar, J. Ai, Structural and functional changes of silk fibroin scaffold due to hydrolytic degradation, J. APPL. POLYM. SCI. 131 (2013) 1–8.
[35] U.J. Kim, J. Park, H.J. Kim, M. Wada, D.L. Kaplan, Three-dimensional aqueous-derived biomaterial scaffolds from silk fibroin, Biomaterials. 26 (2005) 2775–2785.
[36] L.P. Yan, Y.J. Wang, L. Ren, G. Wu, S.G. Caridade, J.B. Fan, L.Y. Wang, P.H. Ji, J.M. Oliveira, J.T. Oliveira, J.F. Mano, R.L. Reis, Genipin-cross-linked collagen/chitosan biomimetic scaffolds for articular cartilage tissue engineering applications, Journal of Biomedical Materials Research Part A. 95A (2010) 465–475.
[37] S.N. Park, J.C. Park, H.O. Kim, M.J. Song, H. Suh, Characterization of porous collagen/hyaluronic acid scaffold modified by 1-ethyl-3-(3-dimethylaminopropyl) carbodiimide cross-linking, Biomaterials. 23 (2002) 1205–1212.
[38] M. Goldberg, J. Smith, Cells and extracellular matrices of dentin and pulp: a biological basis for repair and tissue engineering, Crit Rev Oral Biol Med. 15 (2004) 13–27.
[39] G. Zhou, G. Zhang, Z. Wu, Y. Hou, M. Yan, H. Liu, X. Niu, A. Ruhan, Y. Fan, Research on the structure of fish collagen nanofibers influenced cell growth, Journal of Nanomaterials. 2 (2013) 1–6.
[40] S.I. Dworetzky, E.G. Fey, S. Penmant, J.B. Lian, J.L. Stein, G.S. Stein, Progressive changes in the protein composition of the nuclear matrix during rat osteoblast differentiation, Proc. Natl. Acad. Sci. 87 (1990) 4605–4609.